

## Distribution behavior of inorganic constituents in chemical recycling processes of a municipal waste slag

Kohei OMURA<sup>a</sup>, Shinichi SAKIDA<sup>b</sup>, Yasuhiko BENINO<sup>a</sup>, Tokuro NANBA<sup>a, \*</sup>

<sup>a</sup> Graduate School of Environmental Science, Okayama University, 3-1-1 Tsushima-naka, Kita-ku, Okayama 700-8530, Japan

<sup>b</sup> Environmental Management Center, Okayama University, 3-1-1 Tsushima-naka, Kita-ku, Okayama 700-8530, Japan

† Corresponding author.

Graduate School of Environmental Science, Okayama University, 3-1-1 Tsushima-naka, Kita-ku, Okayama 700-8530, Japan. Tel.: +81 862518896; fax: +81 862518910.

E-mail address: tokuro\_n@cc.okayama-u.ac.jp (T. Nanba)

### Abstract

A chemical recycling process of inorganic wastes has been developed, where after vitrifying wastes, the glasses were heat-treated and soaked in an acid, obtaining colorless and transparent SiO<sub>2</sub>-abundant glasses. In the present study, distribution behavior of the constituents such as Si, P, Ti, Al and so on present in a municipal waste slag was examined. According to compositional analyses, the recovered solids after acid treatment consisted of SiO<sub>2</sub>, P<sub>2</sub>O<sub>5</sub> and TiO<sub>2</sub>, suggesting the preferential distribution of P and Ti atoms into SiO<sub>2</sub>-rich phase during phase separation. In high resolution microscopic analyses, however, it was observed that P and Ti atoms were distributed separately from Si atoms, and they were present in the different particles insoluble in the acid. It was finally concluded that the insoluble solids were produced by a dissolution-reprecipitation process, that is, once all the constituents of the vitrified slag were dissolved in the acid, P<sub>2</sub>O<sub>5</sub> and TiO<sub>2</sub> coprecipitated as particles, and TiO<sub>2</sub> was indispensable for the precipitation of P<sub>2</sub>O<sub>5</sub>. SiO<sub>2</sub> also precipitated as particles separately from P- and Ti-containing particles.

### Keywords

Chemical recycling of wastes, Glass, Phase separation, Dissolution-reprecipitation, Elemental mapping

## 1. Introduction

In Japan, municipal wastes are generally incinerated at temperatures higher than 1300°C, being discharged as molten slags. The slags are reused as raw materials of cement and aggregates in concretes. The authors' research group focused attention on the chemical composition, in which the slags had similar composition to the widely-used commercial glasses such as bottles and windows, and a novel recycling method of municipal waste slags has been developed by using phase separation of glass [1]. The phase separation of alkali borosilicate glasses is well known, where the glasses separate into silica rich and alkali-borate rich phases [2,3]. The municipal waste slags consist of SiO<sub>2</sub>, CaO, and Al<sub>2</sub>O<sub>3</sub> as major constituents, and in the slag recycling process [1], B<sub>2</sub>O<sub>3</sub> is added to promote phase separation. The slag glasses are heat-treated and subsequently soaked in acid solution, obtaining silica rich solids. At this time, coloring components such as Fe<sub>2</sub>O<sub>3</sub> and S are almost completely dissolved in the acid solution, and hence the recovered solids are colorless and transparent. It is also found that, among the slag constituents, P<sub>2</sub>O<sub>5</sub> and TiO<sub>2</sub> seem to be preferentially distributed to the silica rich phase [4].

It has been already demonstrated that phase separation of glass is effective for the recovery of SiO<sub>2</sub> present in inorganic substances such as waste glasses [5] and a blast furnace slag [6], and it is expected that the recovered SiO<sub>2</sub> is used as raw materials of commercial glasses. In addition, if P<sub>2</sub>O<sub>5</sub> and TiO<sub>2</sub> were recovered from wastes, it would be helpful for the industries in resource-poor Japan. In particular, phosphorus has attracted a lot of attention as one of the most necessary resources in Japan, because Japan is totally dependent on imports for phosphate minerals. Thus, recovery and recycling of P<sub>2</sub>O<sub>5</sub> from inorganic wastes are important for the establishment of resource recycling society.

However, little is known about distribution behavior of minor constituents due to phase separation of glasses. Then, our research group has focused on the distribution behavior of P<sub>2</sub>O<sub>5</sub> and TiO<sub>2</sub>, and distribution of P<sub>2</sub>O<sub>5</sub> due to phase separation of Na<sub>2</sub>O-B<sub>2</sub>O<sub>3</sub>-SiO<sub>2</sub> glass has been studied [7-9], where it is found that P<sub>2</sub>O<sub>5</sub> is preferentially distributed to alkali-borate rich phase, and Al<sub>2</sub>O<sub>3</sub> or TiO<sub>2</sub> addition, however, leads to the opposite P<sub>2</sub>O<sub>5</sub> distribution to silica rich phase. In the present study, therefore, it was intended to clarify the distribution of P<sub>2</sub>O<sub>5</sub>, TiO<sub>2</sub> and the other constituents present in the municipal waste slags due to phase separation. Transmission electron microscopy (TEM) observation had been introduced to elucidate the

distribution mechanism of  $P_2O_5$  and  $TiO_2$ , and the experimental findings were, however, somewhat different from the expectations.

## 2. Experimental

### 2.1. Sample preparation

Recycling procedure of municipal waste slags is shown in Fig. 1. The municipal waste slag used in this study was discharged from a waste incineration plant in Okayama prefecture. The powdered slag (abbreviated to S) was mixed with a reagent of  $B_2O_3$  (abbreviated to B) at weight ratios of 10:0, 9:1, 8:2 (designated as S10B0, S9B1 and S8B2, respectively), and the mixtures were melted at  $1400^\circ\text{C}$  for 1 hour in a Pt crucible. The melts were then press-quenched on a steel plate, obtaining the slag glasses. In the previous study [1], the slags were melted at  $1500^\circ\text{C}$  for 0.5 hours, and in the present study, different melting condition was chosen. It is due to the following reason: in the previous study, phase separation could not be confirmed in scanning electron microscope (SEM) observations. If liquid-liquid phase separation takes place in the molten slags, lower melting temperature and longer melting time are appropriate to induce liquid-liquid phase separation. Then, in this study, the melting condition of  $1400^\circ\text{C}$  for 1 hour was applied to the slags.

For comparison, a glass with composition of  $10Na_2O \cdot 40B_2O_3 \cdot 41SiO_2 \cdot 3Al_2O_3 \cdot 3P_2O_5 \cdot 3TiO_2$  (mol%) was also prepared by a conventional melt-quenching method, which is the same composition with the sample A3T3 in the previous paper [9]. The raw materials of reagent grade  $Na_3PO_4 \cdot 12H_2O$ ,  $Na_2CO_3$ ,  $B_2O_3$ ,  $SiO_2$  and  $Al_2O_3$  were mixed thoroughly and heated at  $250^\circ\text{C}$  for 3 hours to remove  $H_2O$  and  $CO_2$ . Then, the mixture was melted at  $1400^\circ\text{C}$  in a Pt crucible for 0.5 hours, and the melt was then press-quenched on a steel plate, obtaining the reference glass (abbreviated to A3T3). In the preparation of A3T3, shorter melting time of 0.5 hours was used. As described later, phase separation is successfully confirmed after the subsequent heat-treatment, and hence 0.5 hours of melting time is enough to prepare the reference specimen.

For the purpose of inducing and progressing phase separation, the glasses were heat-treated at temperatures higher than glass transition temperature,  $T_g$  which was determined with differential thermal

analysis (DTA). The heat-treated glasses were ground into coarse particles ( $< 150 \mu\text{m}$ ), and 1.5 g of the powders were soaked in 2.5 N HCl solution of 20 mL for 24 hours. After vacuum filtration, the insoluble residues were rinsed in water and dried, obtaining the end products and filtrates.

## 2.2. Evaluations

DTA measurement was performed with the powdered glasses ( $< 150 \mu\text{m}$ ) in a Pt pan at a heating rate of  $20^\circ\text{C}/\text{min}$  from room temperature to  $1000^\circ\text{C}$ .

Chemical composition of the solutions as well as the slag glasses and end products was determined by inductively coupled plasma optical emission spectroscopic (ICP-OES) analysis, where solid specimens were completely dissolved in acids and provided for the measurement. Concentration of the elements was estimated with the calibration lines of respective elements, and the relative standard deviation (RSD)  $< 3\%$  was achieved.

Microstructure of the samples was observed by scanning transmission electron microscopy (STEM) operated at an accelerating voltage of 200 kV. When some damages were confirmed, the accelerating voltage was reduced to 120 kV. The STEM apparatus was equipped with energy dispersive X-ray spectrometer (EDX), and elemental mapping was also obtained by the STEM/EDX. For the STEM measurements, the samples were ground into fine powders ( $< 1 \mu\text{m}$ ) or fabricated to thin films (ca. 200 nm) by a focused ion beam (FIB) device. The powdered samples were ultrasonically dispersed in ethanol, and then a few drops of the suspension were put into a carbon-coated Cu microgrid. The reproducibility of chemical composition estimated by STEM/EDX measurement was not confirmed, but STEM/EDX must have poor reproducibility than ICP-OES.

## 3. Results

### 3.1. Distribution in the glasses derived from municipal waste slag

$T_g$ s of S10B0, S9B1 and S8B2 are 730, 680 and  $650^\circ\text{C}$ , respectively.  $\text{B}_2\text{O}_3$  addition leads to the lowering

in  $T_g$ . All samples were colored greenish brown, and no change was observed in color after the heat treatment at  $T_g + 50^\circ\text{C}$  for 24 hours.

Table 1 shows the analytical compositions of the slag glasses estimated with ICP-OES analysis. The analytical values are somewhat different from those given in the previous study [1]. For example,  $\text{SiO}_2$  and  $\text{CaO}$  contents are 35.4 and 36.1 in the previous study, and 40.3 and 30.1 in the present study. In the previous study, an X-ray fluorescence (XRF) apparatus was used. In the XRF apparatus, energy resolution was not so high, and the peaks of neighboring atoms such as Al, Si, P and S were overlapped at bottoms. The ICP-OES apparatus used in the present study prevents such the spectral overlap, and hence the analytical values of ICP-OES in this study should be more accurate than those of XRF in the present study.

In order to investigate the distribution behavior of the constituents, the relative amount of each element remaining in the insoluble solids after acid treatment was calculated from the chemical compositions of the slag glasses before acid treatment and the concentration in the filtrates after acid treatment. The result is shown in Fig. 2, where  $\text{Na}_2\text{O}$ ,  $\text{MgO}$ ,  $\text{Al}_2\text{O}_3$ ,  $\text{CaO}$ ,  $\text{Cr}_2\text{O}_3$ ,  $\text{MnO}$ ,  $\text{Fe}_2\text{O}_3$  and  $\text{ZnO}$  are preferentially dissolved in acid together with  $\text{B}_2\text{O}_3$ . In the case of  $\text{P}_2\text{O}_5$  and  $\text{TiO}_2$ , however, these components remain with  $\text{SiO}_2$  in the end products at relatively high rates. Complete removal of  $\text{Fe}_2\text{O}_3$  from the slag glasses seems to be difficult. Table 1 also shows the calculated chemical compositions of the end products recovered from the slag glasses. The insoluble end products commonly consist of large amount of  $\text{SiO}_2$  (87.1 – 88.5 mass%) and small amounts of  $\text{P}_2\text{O}_5$  (5.3 – 5.7 mass%) and  $\text{TiO}_2$  (4.9 – 5.3 mass%).

STEM and STEM/EDX elemental mapping images of S9B1 are shown in Fig. 3. In Fig. 3a, the slag glass S9B1 after heat treatment was milled into thin film with ca. 200 nm thickness by FIB. In the STEM measurements, a 200 kV of accelerating voltage was applied to both samples. Table 2 shows the chemical compositions of the specified regions in Fig. 3b analyzed by EDX. Characteristic X-rays of  $K\alpha$  beams, Al, Si, P, Ca, Ti and Fe were picked out, but B  $K\alpha$  beam could not be detected.

The specimens derived from the slag glasses were easily damaged at higher magnifications, and hence the observations only at lower resolutions were achieved at 200 kV. In Fig. 3a, neither difference in contrast nor elemental inhomogeneity is observed, and that is, phase separation is not confirmed at the resolution given in Fig. 3a. After acid treatment, particles with various sizes are confirmed, and elemental inhomogeneity is clearly observed in Fig. 3b. Si is present in larger particles (ca. 800 nm), and on the contrary, P and Ti are

identified in the same particles smaller than the Si-containing particles. In the smaller particles, furthermore, P and Ti are accompanied by small amount of Fe, Al and Ca. These results suggest that Si is distributed separately from P and Ti to the insoluble end products.

### 3.2. Distribution in the sodium borosilicate glass

The reference glass A3T3, which was colorless and transparent, was heat-treated at 600°C for 16 hours, and the glass changed into white and opaque. Table 3 shows the chemical composition of the end products recovered from A3T3 and the remaining rate of each constituent after acid treatment. The remaining rates for A3T3 are similar to those for the slag glasses given in Fig. 2. In the case of Al<sub>2</sub>O<sub>3</sub>, however, the remaining rate is somewhat different.

STEM and STEM/EDX elemental mapping images of the powdered A3T3 before and after acid treatment are shown in Fig. 4, where the measurements were performed at 120 kV. Before acid treatment (Fig. 4a), spherical droplets of ca. 50 – 100 nm in diameter are observed in the continuous matrix phase, suggesting a phase separation due to the nucleation and growth mechanism [10]. Inhomogeneity is also confirmed in the elemental mapping images. Chemical composition of the regions specified in Fig. 4 is listed in Table 4. Concentrations of Na<sub>2</sub>O, P<sub>2</sub>O<sub>5</sub> and TiO<sub>2</sub> in a droplet (region 2 in Fig. 4a) are larger than those in the matrix (region 1 in Fig. 4a). However, SiO<sub>2</sub> concentration in the matrix is higher than the droplet. These results suggest that the droplets are B<sub>2</sub>O<sub>3</sub>-rich phase, and P and Ti are distributed to the B<sub>2</sub>O<sub>3</sub>-rich phase due to phase separation. The experimental facts are contrary to the expectations.

After acid treatment of A3T3 (Fig. 4b), particles with various sizes are seen. SiO<sub>2</sub> is abundant in larger particles (ca. 100 nm), and P<sub>2</sub>O<sub>5</sub> and TiO<sub>2</sub> are found in the same smaller particles. The elemental distribution of Si, P and Ti in Fig. 4b is similar to that of the slag glass in Fig. 3b, that is, in the region where P and Ti are abundant, Si is poorly distributed. In the case of Al, however, the distribution is somewhat different between S9B1 and A3T3.

## 3. Discussion

As shown in Table 1 and Fig. 2, the chemical composition of the end products and elemental remaining rate are almost independent of  $B_2O_3$  content added to the slag. In the previous paper [1], similar result was already reported, and small dependency on the heat-treatment was also described. At that time, two mechanisms were supposed, that is, liquid-liquid phase separation in vitrification process and dissolution-reprecipitation in acid treatment, but conclusive evidences could not be obtained. As shown in Fig. 3a, the STEM/EDX images indicate homogeneous elemental distribution, suggesting that no phase separation takes place even after the heat treatment. However, STEM/EDX observations at higher magnifications are not applicable to the specimens prepared in the present study, and hence, the possibility of liquid-liquid phase separation is not completely denied. In A3T3 with a simplified glass composition, phase separation is surely confirmed (Fig. 4a), and the mechanism suggested is not the spinodal decomposition but the nucleation and growth process.

If it is assumed that insoluble solids are formed by dissolution-reprecipitation mechanism, it is expected that the concentrations of the constituents in acid solution once increase by the dissolution process and then decrease by the reprecipitation process. Hence, ICP measurements were repeated with changing the soaking time. Fig. 5 shows the dissolution rates of the constituents in S9B1 slag glass, where a steep increase in the dissolution rate is commonly observed at the soaking time  $< 2$  hours, and the dissolution rate reaches equilibrium at around 10 hours. As for  $SiO_2$  and  $TiO_2$ , a gradual decrease in the dissolution rate is commonly observed at 2 – 16 hours, which strongly suggests the reprecipitation process. The change of  $P_2O_5$  is somewhat different from those of other constituents.

It was also considered in the previous paper [1] that P and Ti preferred to be dissolved in  $SiO_2$ -rich phase. As shown in Fig. 3b, however, the STEM/EDX images show that  $SiO_2$  is distributed separately from  $P_2O_5$  and  $TiO_2$  in the insoluble end product, suggesting that P and Ti are not incorporated into  $SiO_2$ -rich glass matrix constituting the end products. As also suggested from Fig. 4, P and Ti are distributed to  $B_2O_3$ -rich phase rather than  $SiO_2$ -rich phase due to phase separation. If P and Ti are homogeneously present in the  $B_2O_3$ -rich phase which is soluble in acidic solution, P and Ti are also dissolved in the acidic solution together with  $B_2O_3$ -rich phase. However, P and Ti are confirmed in the insoluble end products, indicating that P and Ti coprecipitate in acid.

Table 5 shows the change in P/Ti atomic ratio. In the glasses before acid treatment, P/Ti ratio is 1.8 – 2.0, and in the end products after acid treatment, P/Ti ratio decreases to 1.0 – 1.3. The ratio may have some meaning such as formation ability of P- and Ti-containing crystals insoluble in acid. In the Al- and Ti-free sodium borosilicate glasses, P is dissolved in acid and not present in insoluble solids [7-9], indicating that P is originally soluble in acid solution. It is therefore supposed that P is incorporated in TiO<sub>2</sub> particles formed by the reprecipitation process, and the P/Ti ratio of 1.0 – 1.3 is probably the upper limit of coprecipitated substances. In Fig. 5, the dissolution rate curve of P is different from that of Ti, which is due to the presence of residual P not incorporated in the TiO<sub>2</sub>-based precipitates. Currently, the mechanisms of P and Ti coprecipitation and the separate Si precipitation are poorly understood, and further investigations are required.

#### 4. Conclusion

Distribution behavior of the glass constituents derived from the municipal waste slag was investigated. Preferential distributions of P and Ti into SiO<sub>2</sub>-rich phase and the other constituents into B<sub>2</sub>O<sub>3</sub>-rich phase had been suggested in the ICP-OES compositional analyses. In STEM/EDX observations, however, phase separation of the slag glasses even after heat treatment could not be confirmed, suggesting that the insoluble solids after acid treatment were formed with dissolution-reprecipitation process. The STEM/EDX observations also revealed that P and Ti were distributed separately from Si in the precipitated particles, and the similar results were also found in the sodium borosilicate glass containing Al, P and Ti. In the borosilicate glass, furthermore, P and Ti were found in B<sub>2</sub>O<sub>3</sub>-rich phase after phase separation. Just after a slag glass was soaked in acid, concentration of Si and Ti dissolved in acid increased steeply and then decreased gradually. It was finally concluded that SiO<sub>2</sub> and TiO<sub>2</sub> insoluble particles were separately formed in acid by dissolution-reprecipitation process, and P was incorporated in the TiO<sub>2</sub> particles by coprecipitation up to P/Ti atomic ratio of 1.0 – 1.3.



## Acknowledgment

The authors would like to thank Dr. H. Hashimoto of Okayama University for the technical supports in STEM observations.

## References

- [1] T. Nanba, Y. Kuroda, S. Sakida and Y. Benino, *J. Ceram. Soc. Japan*, 117, 1195-1198 (2009).
- [2] W. Haller, D.H. Blackburn, F.E. Wagstaff and R.J. Charles, *J. Am. Ceram. Soc.*, 53, 34-39 (1970).
- [3] O.V. Mazurin and M.V. Streltsina, *J. Non-Cryst. Solids*, 11, 199-218 (1972).
- [4] K. Omura, S. Sakida, Y. Benino and T. Nanba, Extended Abstracts in the 28th Japan-Korea International Seminar on Ceramics, p.385 (2011).
- [5] T. Akai, D. Chen, H. Masui, K. Kuraoka and T. Yazawa, “Method for recycling waste glass and recycled glass”, International Patent No. WO/2003/024879 (2003).
- [6] T. Nanba, S. Mikami, T. Imaoka, S. Sakida and Y. Miura, *J. Ceram. Soc. Japan*, 116, 220-223 (2008).
- [7] Y. Ohtsuki, S. Sakida, Y. Benino and T. Nanba, IOP Conf. Series: Materials Science and Engineering 18, 112022, (2011) doi:10.1088/1757-899X/18/11/112022.
- [8] Y. Ohtsuki, S. Sakida, Y. Benino and T. Nanba, Processing, Properties, and Applications of Glass and Optical Materials: Ceramic Transactions, 231, 145-149 (2012).
- [9] Y. Benino, Y. Ohtsuki, S. Sakida, and T. Nanba, *J. Ceram. Soc. Japan*, 120, 490-493 (2012).
- [10] N.S. Andreev, E.A. Porai-Koshits and O.V. Mazurin, in “Phase Separation in Glass”, Ed. by O.V. Mazurin and E.A. Porai-Koshits, North-Holland Physics Publishing, New York, (1984) Chap. III, pp. 67-101.

## Figure captions

**Fig. 1.** Recycling procedure used in the present study.

**Fig. 2.** Remaining rate of elements in the end products insoluble in acid.

**Fig. 3.** STEM and STEM/EDX elemental mapping images of S9B1 before (a) and after (b) acid treatment. Chemical composition in the regions 1 and 2 is listed in Table 2.

**Fig. 4.** STEM and STE/EDX elemental mapping images of A3T3 before (a) and after (b) acid treatment. Chemical composition in the regions 1 – 4 is listed in Table 4.

**Fig. 5.** Dissolution rate of the constituents in S9B1 soaked in acid. The lines are drawn as guides to the eye.

## Tables

**Table 1.** ICP-OES analytical composition (mass%) of the slag glasses before acid treatment and insoluble end products after acid treatment.

Sample	Slag glass			End product		
	S10B0	S9B1	S8B2	S10B0	S9B1	S8B2
B <sub>2</sub> O <sub>3</sub>	0.0	9.2	18.8	0	0	0.3
Na <sub>2</sub> O	1.6	1.7	1.6	0	0	0
MgO	2.8	2.6	2.3	0.1	0.1	0
Al <sub>2</sub> O <sub>3</sub>	16.1	14.4	13.4	0.5	0.6	0
SiO <sub>2</sub>	37.7	33.6	30.2	87.1	87.9	88.5
P <sub>2</sub> O <sub>5</sub>	3.0	2.7	2.5	5.7	5.3	5.6
CaO	28.1	25.9	24.6	0.5	0.7	0
TiO <sub>2</sub>	1.9	1.7	1.5	5.3	4.9	4.9
Cr <sub>2</sub> O <sub>3</sub>	0.2	0.2	0.1	0.1	0	0
MnO	0.1	0.1	0.1	0	0	0
Fe <sub>2</sub> O <sub>3</sub>	1.6	1.4	1.2	0.7	0.6	0.6
ZnO	0.2	0.2	0.2	0	0	0
others *	6.6	6.3	3.3	--	--	--

\* total contents of the compounds < 0.1 mass%, such as S, K<sub>2</sub>O, CuO and PbO.

**Table 2.** Chemical composition (mass%) of the regions specified in Fig. 3b obtained from STEM/EDX observation of S9B1.

	Al <sub>2</sub> O <sub>3</sub>	SiO <sub>2</sub>	P <sub>2</sub> O <sub>5</sub>	CaO	TiO <sub>2</sub>	Fe <sub>2</sub> O <sub>3</sub>
Region 1	0	99.5	0	0.1	0.4	0
Region 2	2.8	19.1	31.7	1.7	40.6	4.2

**Table 3.** Chemical composition of the end product obtained from A3T3 and remaining rate of constituents estimated from ICP-OES analyses.

	Na <sub>2</sub> O	B <sub>2</sub> O <sub>3</sub>	SiO <sub>2</sub>	Al <sub>2</sub> O <sub>3</sub>	P <sub>2</sub> O <sub>5</sub>	TiO <sub>2</sub>
Composition (mol%)	1.1	4.5	81.7	1.2	3.7	7.7
Remaining rate (%)	3.2	4.7	88.8	16.2	44.6	94.9

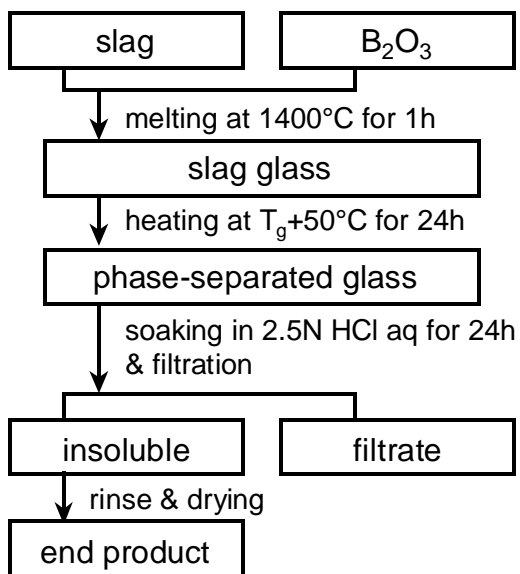
**Table 4.** Chemical composition (mol%) of the regions specified in Fig. 4 obtained from STEM/EDX observation of A3T3.

	Na <sub>2</sub> O	Al <sub>2</sub> O <sub>3</sub>	SiO <sub>2</sub>	P <sub>2</sub> O <sub>5</sub>	TiO <sub>2</sub>
a) before acid treatment					
Region 1	0	4.7	87.3	4.0	4.0
Region 2	4.9	5.0	58.5	8.4	23.1
b) after acid treatment					
Region 3	0	0	99.0	0.2	0.8
Region 4	0	1.6	53.9	15.0	29.5

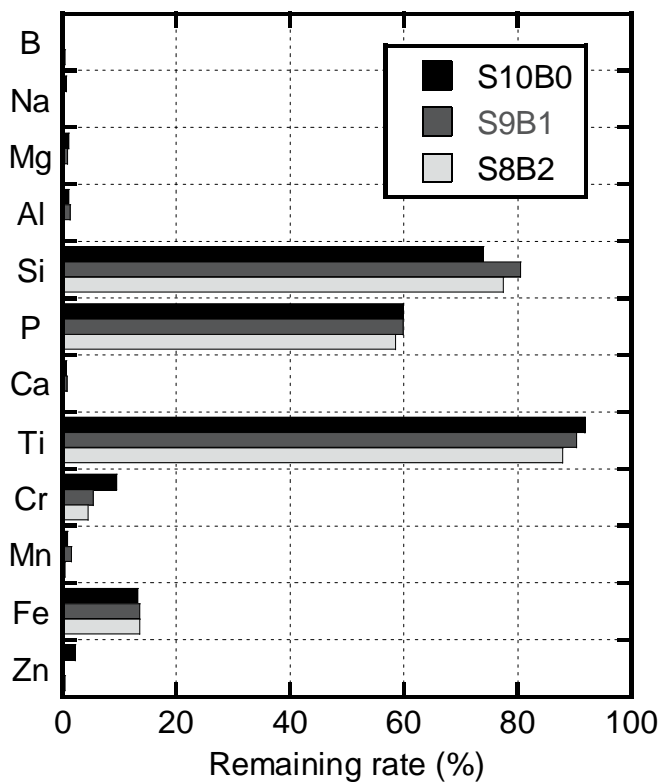
**Table 5.** P/Ti atomic ratio of the glasses before acid treatment and insoluble end products after acid treatment.

Sample	Slag glass	End product
S10B0	1.8	1.2
S9B1	1.9	1.2
S8B2	1.9	1.3
A3T3	2.0	1.0

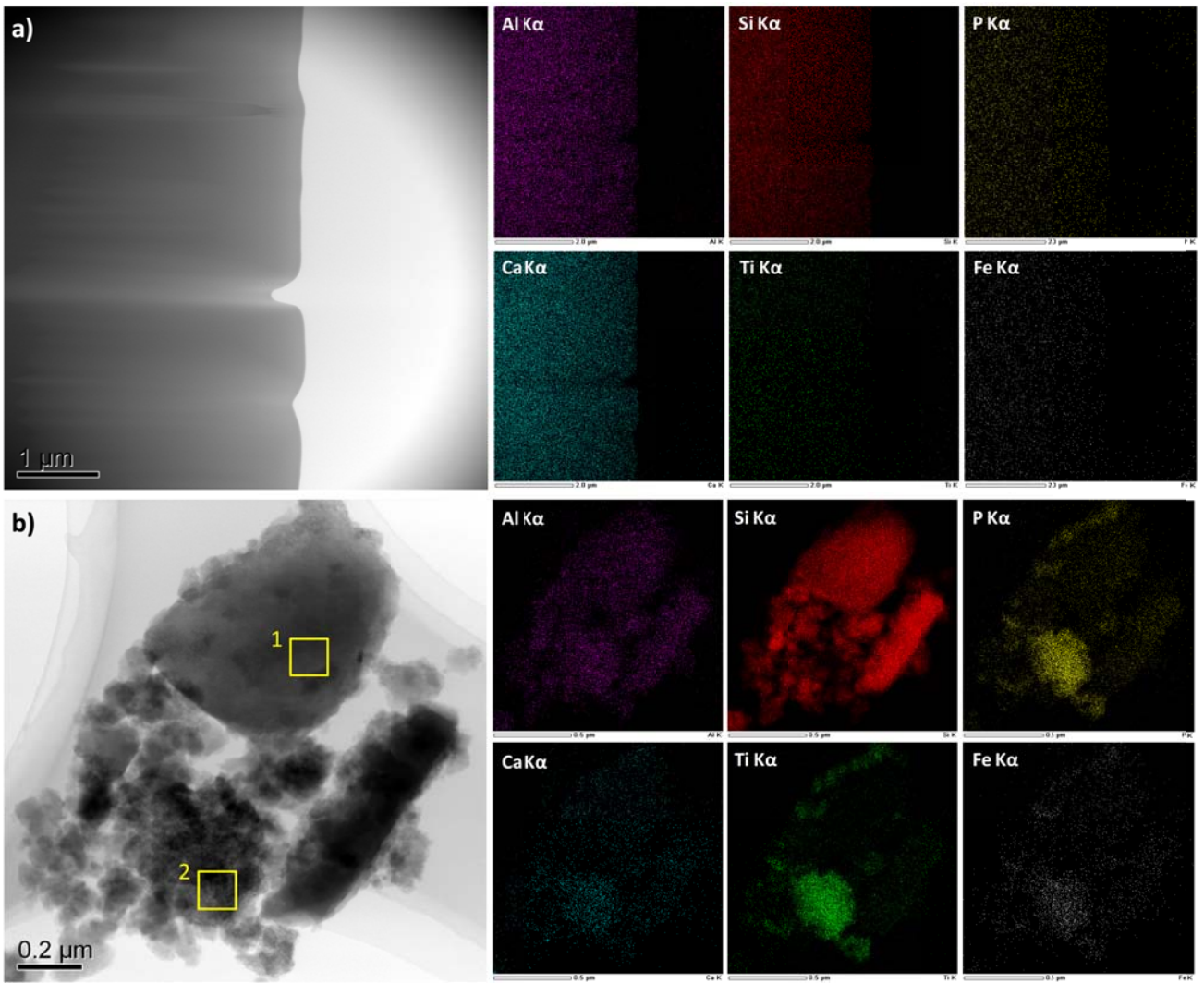
Figures



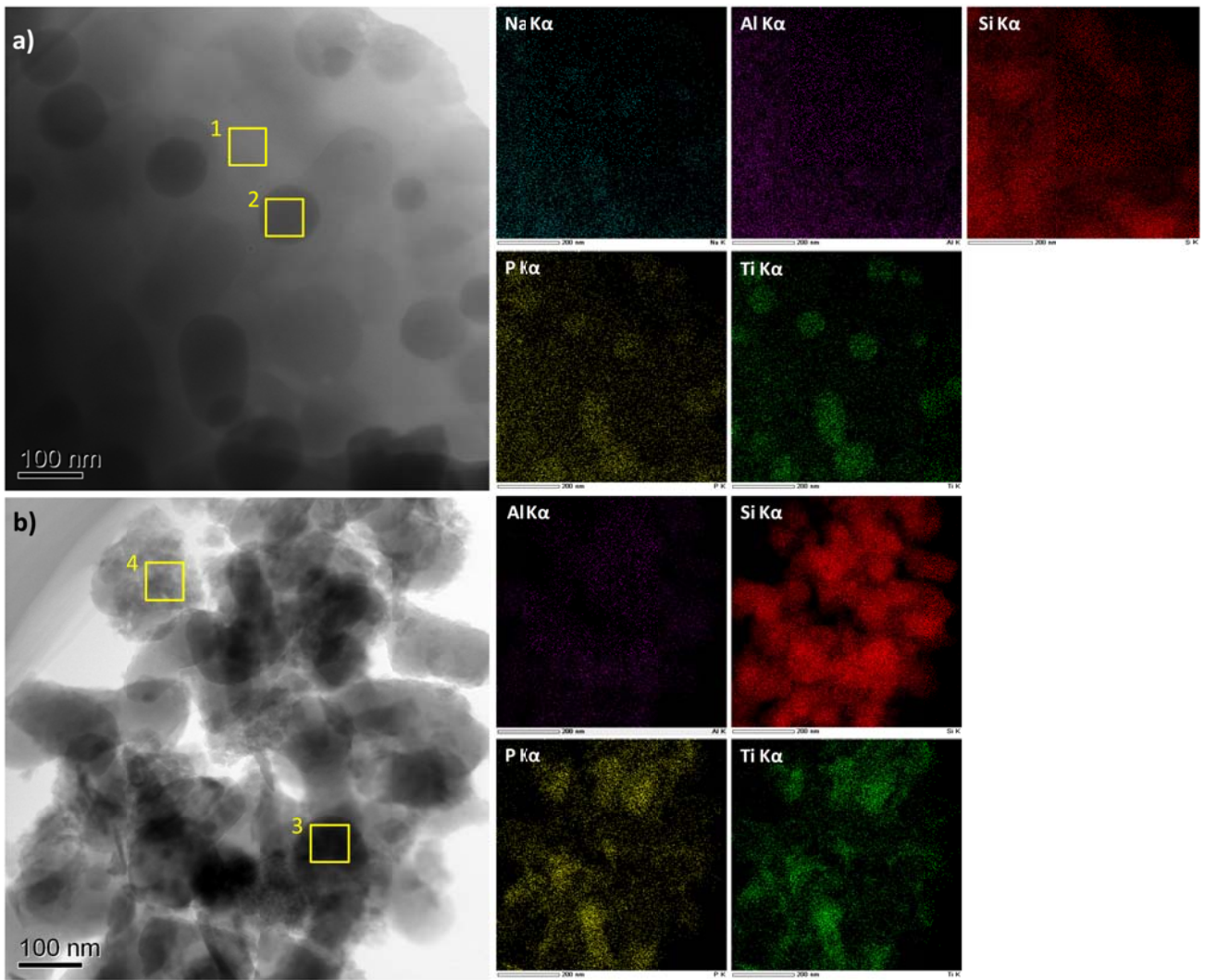
Omura et al., Fig. 1.



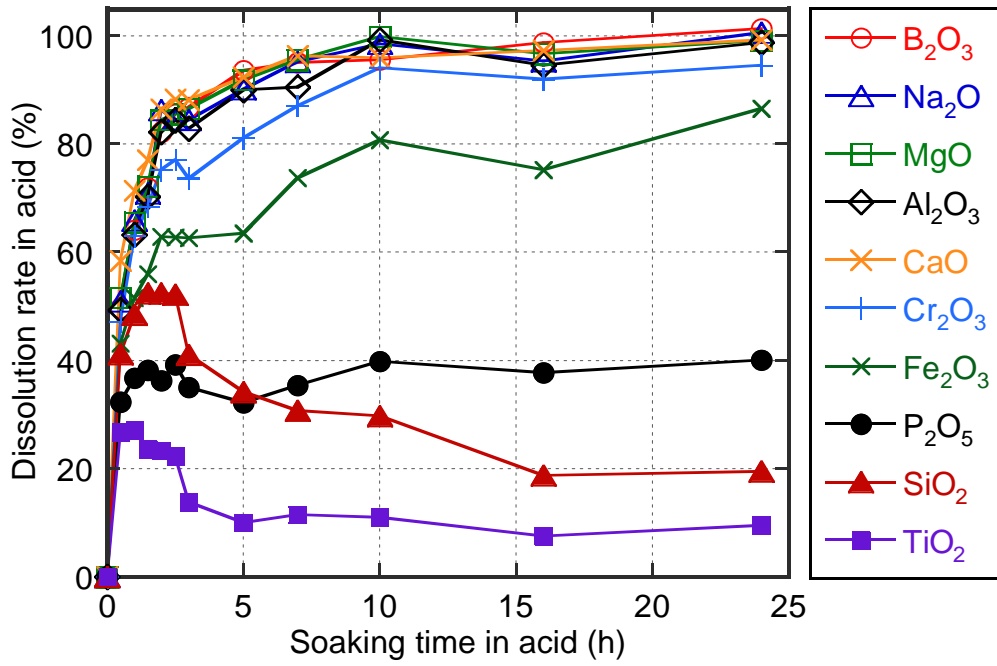
Omura et al., Fig. 2.



Omura et al., Fig. 3.



Omura et al., Fig. 4.



Omura et al., Fig. 5.